The Effect of Communication Topology on Scalar Field Estimation by Large Networks with Partially Accessible Measurements

Ragesh K. Ramachandran[1] and Spring Berman[1]

***Abstract*— This paper studies the problem of reconstructing a two-dimensional scalar field using measurements from a subset of a network with local communication between nodes. We consider the communication network of the nodes to form either a chain or a grid topology. We formulate the reconstruction problem as an optimization problem that is constrained by first-order linear dynamics on a large interconnected system. To solve this problem, we employ an optimization-based scheme that uses a gradient-based method with an analytical computation of the gradient. The main contribution of the paper is a derivation of bounds on the trace of the observability Gramian of the system, which can be used to quantify and compare the field estimation capabilities of chain and grid networks. A comparison based on a performance measure related to the $\mathscr{H}_2$ norm of the system is also used to study the robustness of the network topologies. Our results are validated in simulation using both Gaussian scalar fields and actual ocean salinity data.**

***Index Terms*— Networked robotic systems, sensor networks, field estimation.**

I. INTRODUCTION

Large networks of robots or sensors, hereafter referred to generally as *nodes*, can perform a range of distributed sensing and estimation tasks such as environmental monitoring, field surveillance and reconstruction, multi-target tracking, and geo-scientific exploration [1], [2], [3]. The environment to be sampled by the network may be remote or hazardous, allowing measurements to be directly accessed from only a subset of the nodes at any given time. Our primary motivation in this paper is to quantify the fundamental performance limitations that emerge in these scenarios due to the chosen *inter-node communication topology* of the network. This topology can be implemented in stationary networks through the configuration of the nodes and enforced in mobile networks using strategies such as formation control [4] and traffic control for platoons [5].

Toward this end, we investigate the effect of network topology on the accuracy and robustness of a method that we devise for reconstructing a static scalar field from partial observations. We note that our method can also be adapted to estimate a time-varying scalar field whose dynamics are slower than the network information dynamics. This method uses temporal data collected by the accessible nodes in the network to estimate the initial measurements of the field that were obtained by the full set of nodes. The nodes share their measurements with their neighbors through a fixed communication network. The network is assigned either a grid or chain topology, which are common candidates for approximating 1D and 2D domains in practical applications. We specify that the information flow in the network is governed by a first-order linear dynamical model. This simple model of information dynamics represents the case where no data is stored in the nodes and a single item of information is transmitted between nodes at a time. In addition, this model yields diffusive information dynamics that eventually approach a steady state, which allows us to determine a time at which the data values at the nodes have largely stabilized and thus gives a fixed time interval over which the data can be retrieved. From a control theory perspective, the estimation problem addressed by our method is equivalent to finding the initial condition of a linear dynamical system given its inputs and outputs. The solution to this problem is associated with the *observability* of the system.

Although there is a great deal of literature on optimal control, little work has addressed the optimal estimation of initial conditions other than through the inversion of the observability Gramian [6]. In general, the observability of a linear dynamical system can be verified by using the Kalman rank condition [7]. However, checking the rank condition for large interconnected systems is computationally intensive due to the high dimensionality of the observability Gramian. For this reason, a less computationally intensive graph-theoretic characterization of observability has been more widely used than a matrix-theoretic characterization for large complex networked systems. The observability of complex networks is studied in [8] using a graph-based approach, which presents a general result that holds true for most of the chosen network parameters (the edge weights). In [9], a graph-theoretic approach based on equitable partitions of graphs is used to derive necessary conditions for observability of networks. Alternately, [10] uses a matrix-theoretic approach to develop a maximum multiplicity theory to characterize the exact controllability of a network in terms of the minimum number of required independent controller nodes based on the network spectrum.

We adopt a quantitative measure of observability, based on the trace of the observability Gramian, that is similar to [11], [12], [13], [14], [15], departing from the graph-theoretic methods used in [9], [8], [16], [17]. Our analysis makes use of necessary and sufficient conditions for the observability spectral properties of chain and grid networks, which are well-understood [16], [18]. In the main result of

This work was supported by National Science Foundation (NSF) award no. CMMI-1363499.

[1]Ragesh K. Ramachandran and Spring Berman are with the School for Engineering of Matter, Transport and Energy, Arizona State University, Tempe, AZ 85287, USA rageshkr@asu.edu, spring.berman@asu.edu

this paper, we derive bounds on the trace of the observability Gramian of an undirected network and use these bounds to compare the estimation performance of networks with either grid or chain topologies. We evaluate this performance for our novel method of estimating the initial condition of a large network with linear dynamics, which constitutes another contribution of this paper. We use an optimization framework to address this estimation problem and derive the gradient required to solve it. A third contribution of the paper is our characterization of a network's robustness to noise using a performance measure based on the $\mathscr{H}_2$ norm of the system. We find that even with simple first-order information dynamics, the topology of the network significantly affects its estimation performance and its robustness to noise. We illustrate our approach on both simulated and actual two-dimensional scalar fields.

The paper is organized as follows. Section II introduces relevant mathematical concepts and terminology. Section III describes the problem statement and outlines the assumptions made in its formulation. The network model is presented in Section IV. Section V delineates how the scalar field reconstruction can be posed as an optimization problem and computes the analytical gradient required for its solution. Simulation details and results are described in Section VI. We derive bounds on the trace of the observability Gramian in Section VII, which aids us in comparing network topologies. Section VIII discusses a performance analysis of the network topologies based on the $\mathscr{H}_2$ norm of the system. Finally, Section IX concludes the paper and proposes future work.

II. MATHEMATICAL PRELIMINARIES

A graph $\mathscr{G}$ can be defined as the tuple $(V(\mathscr{G}),E(\mathscr{G}))$, where $V(\mathscr{G})$ is a set of N vertices, or *nodes*, and $E(\mathscr{G}) = \{(i,j) : i \neq j,\ i,j \in V(\mathscr{G})\}$ is a set of M *edges*. Nodes i and j are called *neighbors* if $(i,j) \in E(\mathscr{G})$. The set of neighbors of node i is denoted by $\mathscr{N}_i = \{j : j \in V(\mathscr{G}),(i,j) \in E(\mathscr{G})\}$. The *degree* d_i of a node i is defined as $|\mathscr{N}_i|$. We assume that $\mathscr{G}$ is finite, simple, and connected unless mentioned otherwise.

A graph $\mathscr{G}$ is associated with several matrices whose spectral properties will be used to derive our results. The *incidence matrix* of a graph with arbitrary orientation is defined as $\mathbf{B}(\mathscr{G}) = [b_{ij}] \in \mathbb{R}^{N\times M}$, where the entry $b_{ij} = 1$ if i is the initial node of some edge j of $\mathscr{G}$, $b_{ij} = -1$ if i is the terminal node of some edge j of $\mathscr{G}$, and $b_{ij} = 0$ otherwise. It can be shown that the left nullspace of $\mathbf{B}(\mathscr{G})$ is $c\mathbf{1}_N,\ c \in \mathbb{R}$, where $\mathbf{1}_N$ is the $N \times 1$ vector of ones [19]. The *degree matrix* $\Delta(\mathscr{G})$ of a graph is given by $\Delta(\mathscr{G}) = Diag(d_1,...,d_N)$. The *adjacency matrix* $\mathbf{A}(\mathscr{G}) = [a_{ij}] \in \mathbb{R}^{N\times N}$ has entries $a_{ij} = 1$ when $(i,j) \in E(\mathscr{G})$ and $a_{ij} = 0$ otherwise. The *graph Laplacian* can be defined from these two matrices as $\mathbf{L}(\mathscr{G}) = \Delta(\mathscr{G}) - \mathbf{A}(\mathscr{G})$. The Laplacian of an undirected graph is symmetric and positive semidefinite, which implies that it has real nonnegative eigenvalues $\lambda_i(\mathscr{G})$, $i = 1,...n$. The eigenvalues can be ordered as $\lambda_1(\mathscr{G}) \leq \lambda_2(\mathscr{G}) \leq ... \leq \lambda_N(\mathscr{G})$, where $\lambda_1(\mathscr{G}) = 0$. The eigenvector corresponding to eigenvalue $\lambda_1(\mathscr{G})$ can be computed to be $\mathbf{1}_N$. By Theorem 2.8 of [20], the graph is connected if and only if $\lambda_2(\mathscr{G}) > 0$.

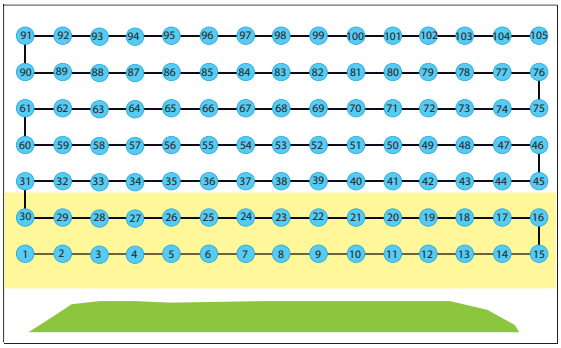

(a) Chain topology

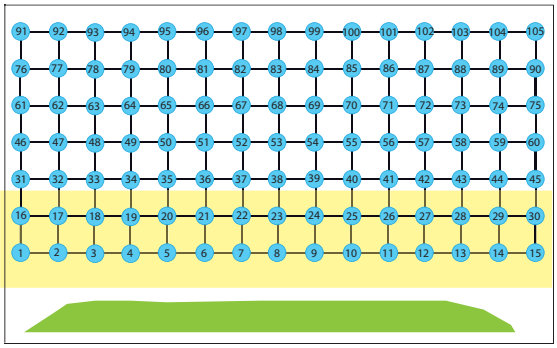

(b) Grid topology

Fig. 1. Illustration of the chain and grid network topologies. The blue circles are nodes and are labeled by numbers. Nodes in the yellow region are accessible nodes.

Several other matrices will be defined as follows. An $n_1 \times n_2$ identity matrix will be denoted by $\mathbf{I}_{n_1\times n_2}$, and an $n_1 \times n_2$ matrix of zeros will be denoted by $\mathbf{0}_{n_1\times n_2}$. The matrix $\mathbf{J}_N$ is defined as $\mathbf{J}_N = \mathbf{1}_N^T\mathbf{1}_N$.

III. PROBLEM STATEMENT

Consider a set of N nodes with local communication ranges and local sensing capabilities. The nodes are arranged in a bounded domain as shown in Figure 1. Each node is capable of measuring the value of a scalar field at its location and communicating this value to its neighbors, which are defined as the nodes that are within its communication range. The nodes take measurements at some initial time and transmit this information using a nearest-neighbor averaging rule, which is described in Section IV. As shown in Figure 1, we assume to have direct access only to the measurements of a small subset of the nodes, which we call the *accessible nodes*, which for instance may be closer to a particular boundary of the domain. We also assume that the node positions are predetermined and that the nodes employ feedback mechanisms to regulate their positions in the presence of external disturbances.

We address the problem of reconstructing the initial measurements taken by all the nodes from the measurements of the accessible nodes. This can be formulated as the problem of determining whether the information flow dynamics in the network are observable with respect to a set of given outputs. As discussed in Section I, we restrict our investigation to

chain and grid communication topologies, whose structural observability properties are well-studied [16], [17]. We will focus on comparing the chain and grid topologies in terms of their utility as communication networks to be used in reconstructing an initial set of data.

IV. NETWORK MODEL

The communication network among the N nodes is represented by an undirected graph $\mathscr{G} = (V(\mathscr{G}), E(\mathscr{G}))$, where vertex $i \in V(\mathscr{G})$ denotes node i, and nodes i and j can communicate with each other if $(i,j) \in E(\mathscr{G})$. Let $x_i(t) \in \mathbb{R}$ be a scalar data value obtained by node i at time t. We define the information flow dynamics of node i as

$$\frac{dx_i}{dt} = \sum_{(i,j)\in\mathscr{N}_i} (x_j - x_i). \tag{1}$$

The vector of all nodes' information at time t is denoted by $\mathbf{X}(t) = [x_1(t)\ x_2(t)\ \ldots\ x_N(t)]^T$. Using Equation (1) to define the dynamics of $x_i(t)$ for each node i, we can define the information flow dynamics over the entire network as

$$\begin{aligned} \dot{\mathbf{X}}(t) &= -\mathbf{L}(\mathscr{G})\mathbf{X}(t), \\ \mathbf{X}(0) &= \mathbf{X}_0, \end{aligned} \tag{2}$$

where $\mathbf{X}_0 \in \mathbb{R}^N$ contains the unknown initial values of the data obtained by the nodes at time $t = 0$, which is the information that we want to estimate.

We define $Id = \{I_1, I_2, ..., I_k\} \subseteq V(\mathscr{G})$ as the index set of the *accessible nodes*. The output equation for the linear system Equation (2) is given by

$$\mathbf{Y}(t) = \mathbf{C}\mathbf{X}(t), \tag{3}$$

where $\mathbf{Y}(t) \in \mathbb{R}^k$ and $\mathbf{C} = [c_{ij}] \in \mathbb{R}^{k\times N}$ is a sparse matrix whose entries are defined as $c_{ij} = 1$ if $i = j$ and $i \in Id$, $c_{ij} = 0$ otherwise. If we number the nodes in such a way that the first k output nodes are ordered from 1 to k, then $\mathbf{C} = \begin{bmatrix}\mathbf{I}_{k\times k}\ \mathbf{0}_{k\times(N-k)}\end{bmatrix}$.

As previously discussed, we focus on the case where the network has a chain or grid communication topology. The type of topology affects the network dynamics through its associated graph Laplacian $\mathbf{L}(\mathscr{G})$. Let $\mathscr{G}_c$ and $\mathscr{G}_g$ represent communication networks with a chain topology and a grid topology, respectively. When the nodes in each network are labeled as shown in Figure 1(a) and Figure 1(b), then it can be shown that $\mathbf{L}(\mathscr{G}_c)$ and $\mathbf{L}(\mathscr{G}_g)$ [18] have the following structures:

$$\mathbf{L}(\mathscr{G}_c) = \begin{bmatrix} 1 & -1 & 0 & \cdots & \cdots & \cdots & \cdots & 0 \\ -1 & 2 & -1 & \ddots & & & & \vdots \\ 0 & -1 & 2 & -1 & \ddots & & & \vdots \\ \vdots & \ddots & \ddots & \ddots & \ddots & \ddots & & \vdots \\ \vdots & & \ddots & \ddots & \ddots & \ddots & \ddots & \vdots \\ \vdots & & & \ddots & -1 & 2 & -1 & 0 \\ \vdots & & & & \ddots & -1 & 2 & -1 \\ 0 & \cdots & \cdots & \cdots & \cdots & 0 & -1 & 1 \end{bmatrix} \tag{4}$$

and

$$\mathbf{L}(\mathscr{G}_g) = \begin{bmatrix} \mathbf{D}_1 & -\mathbf{I} & 0 & \cdots & \cdots & \cdots & \cdots & 0 \\ -\mathbf{I} & \mathbf{D}_2 & -\mathbf{I} & \ddots & & & & \vdots \\ 0 & -\mathbf{I} & \mathbf{D}_2 & -\mathbf{I} & \ddots & & & \vdots \\ \vdots & \ddots & \ddots & \ddots & \ddots & \ddots & & \vdots \\ \vdots & & \ddots & \ddots & \ddots & \ddots & \ddots & \vdots \\ \vdots & & & \ddots & -\mathbf{I} & \mathbf{D}_2 & -\mathbf{I} & 0 \\ \vdots & & & & \ddots & -\mathbf{I} & \mathbf{D}_2 & -\mathbf{I} \\ 0 & \cdots & \cdots & \cdots & \cdots & 0 & -\mathbf{I} & \mathbf{D}_1 \end{bmatrix}, \tag{5}$$

where

$$\mathbf{D}_1 = \begin{bmatrix} 2 & -1 & \cdots & \cdots & 0 \\ -1 & 3 & -1 & & \vdots \\ \vdots & \ddots & \ddots & \ddots & \vdots \\ \vdots & & -1 & 3 & -1 \\ 0 & \cdots & \cdots & -1 & 2 \end{bmatrix},$$

$$\mathbf{D}_2 = \begin{bmatrix} 3 & -1 & \cdots & \cdots & 0 \\ -1 & 4 & -1 & & \vdots \\ \vdots & \ddots & \ddots & \ddots & \vdots \\ \vdots & & -1 & 4 & -1 \\ 0 & \cdots & \cdots & -1 & 3 \end{bmatrix}.$$

Here, $\mathbf{L}(\mathscr{G}_g)$ is a $(l_1 l_2)\times(l_1 l_2)$ matrix and $\mathbf{D}_1, \mathbf{D}_2$ are both $l_1 \times l_1$ matrices, with $l_1 l_2 = N$. Without loss of generality, we assume that the grid is square, meaning that $l_1 = l_2 = l$. We direct the reader to [21] for a numerical example of $L(\mathscr{G}_g)$.

The graph Laplacians $\mathbf{L}(\mathscr{G}_c)$ and $\mathbf{L}(\mathscr{G}_g)$ are constructed based on the numbering of the vertex sets $V(\mathscr{G}_c)$ and $V(\mathscr{G}_g)$ that is shown in Figure 1. Graphs that are constructed by reordering the vertices of the graphs shown in Figure 1 are isomorphic to the graphs in the figure. Isomorphic graphs are also isospectral [22].

Since the system Equation (2) is linear, its solution is [7]

$$\mathbf{X}(t) = \mathbf{e}^{-\mathbf{L}(\mathscr{G})t}\mathbf{X}_0. \tag{6}$$

By combining Equation (3) and Equation (6), we obtain the map between the unknown initial data $\mathbf{X}_0$ and the measured output $\mathbf{Y}(t)$ as

$$\mathbf{Y}(t) = \mathbf{C}\mathbf{e}^{-\mathbf{L}(\mathscr{G})t}\mathbf{X}_0. \tag{7}$$

V. SCALAR FIELD RECONSTRUCTION

The problem of scalar field reconstruction can now be framed as an inversion of the map given by Equation (7). From linear systems theory, the property of *observability* refers to the ability to determine an initial state $\mathbf{X}_0$ from the inputs and outputs of a linear dynamical system [7]. For systems defined by Equation (2) with an associated chain or grid topology, the conditions for observability are well-studied [16]. This ensures that the reconstruction problem can be solved for the types of networks that we consider.

We solve the scalar field reconstruction problem by posing it as an optimization problem. The optimization procedure uses observed data $\hat{\mathbf{Y}}(t)$ from the accessible nodes over the time interval $t \in [0\ T]$ to recover $\mathbf{X}_0$. The goal of the optimization routine is to find the state $\mathbf{X}_0$ that minimizes the normed distance between this observed data, $\hat{\mathbf{Y}}(t)$, and the output $\mathbf{Y}(t)$ computed using Equation (7). Therefore, we can frame our optimization objective as the computation of $\mathbf{X}_0$ that minimizes the functional $J(\mathbf{X}_0)$, defined as

$$J(\mathbf{X}_0) = \frac{1}{2}\int_0^T \left\|\mathbf{Y}(t) - \hat{\mathbf{Y}}(t)\right\|_2^2 dt + \frac{\lambda}{2}\left\|\mathbf{X}_0\right\|^2, \qquad (8)$$

subject to the constraint given by Equation (7). Here, λ is the Tikhonov regularization parameter, which is added to the objective function to prevent $\mathbf{X}_0$ from becoming large due to noise in the data [23].

The convexity of $J(\mathbf{X}_0)$ ensures the convergence of gradient descent methods to its global minima. We use one such method to compute the $\mathbf{X}_0$ that minimizes this functional. The method requires us to compute the gradient of $J(\mathbf{X}_0)$ with respect to $\mathbf{X}_0$. This is done by combining Equation (7) and Equation (8), then taking the Fréchet derivative of the resulting expression with respect to $\mathbf{X}_0$ [24]. Defining $\Psi(t) = \mathbf{C}e^{-\mathbf{L}(\mathscr{G})t}$, the gradient of $J(\mathbf{X}_0)$ can be computed in this way as:

$$\delta J(\mathbf{X}_0) = \int_0^T \left(\Psi(t)\right)^* \left(\Psi(t)\mathbf{X}_0 - \hat{\mathbf{Y}}(t)\right) dt + \lambda \mathbf{X}_0, \qquad (9)$$

where $(\Psi(t))^*$ is the Hermitian adjoint of $\Psi(t)$, which in this case is simply the Hermitian transpose [24].

The most computationally intensive part of calculating Equation (9) is computing the matrix exponential in $\Psi(t)$. There has been a great deal of literature about approximate computation of the matrix exponential [25], [26], which by definition is an infinite matrix series. In general, finding the matrix exponential is a computationally hard problem for very large matrices and computing it can be error-prone if not done carefully, especially if spectral decomposition [27] of the matrix is not possible [28]. We can calculate the gradient by noting that $\mathbf{Y}(t) = \Psi(t)\mathbf{X}_0$ by Equation (7), applying a change of variables $\tau = T - t$ to the integral term in Equation (9), and defining $\hat{u}(\tau) \equiv \mathbf{Y}(T-\tau) - \hat{\mathbf{Y}}(T-\tau)$:

$$\begin{aligned}
&\int_0^T \left(\Psi(t)\right)^* \left(\Psi(t)\mathbf{X}_0 - \hat{\mathbf{Y}}(t)\right) dt \\
&= \int_0^T \left(\Psi(T-\tau)\right)^* \left(\mathbf{Y}(T-\tau) - \hat{\mathbf{Y}}(T-\tau)\right) d\tau \\
&= \int_0^T \mathbf{e}^{-\mathbf{L}^*(\mathscr{G})(T-\tau)} \mathbf{C}^* \hat{u}(\tau) d\tau.
\end{aligned}$$

This expression can be thought of as the solution $P(\tau)$ of the following differential equation at time $\tau = T$ [7]:

$$\frac{dP}{d\tau} = -\mathbf{L}^*(\mathscr{G})P(\tau) + \mathbf{C}^*\hat{u}(\tau), \quad P(0) = 0. \qquad (10)$$

Using this result, the gradient Equation (9) can be written as

$$\delta J(\mathbf{X}_0) = P(T) + \lambda \mathbf{X}_0. \qquad (11)$$

To compute the gradient, we can solve Equation (10) forward to find $P(T)$.

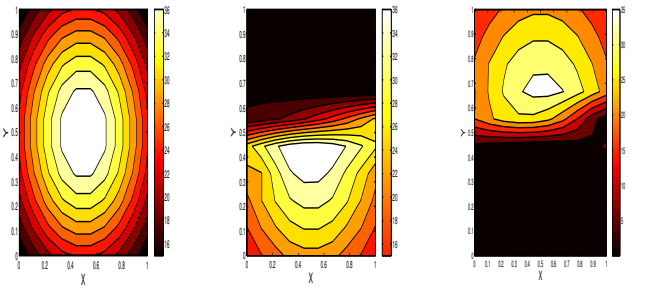

(a) Actual field (b) Estimated field (c) Absolute value of error

Fig. 2. Gaussian function estimation using 100 nodes with a chain communication topology. Temporal data is acquired from 30 nodes over a time period of 50 sec.

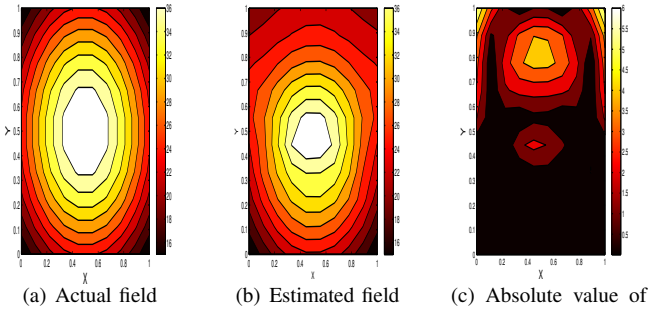

(a) Actual field (b) Estimated field (c) Absolute value of error

Fig. 3. Gaussian function estimation using 100 nodes with a grid communication topology. Temporal data is acquired from 30 nodes over a time period of 50 sec.

VI. SIMULATIONS

We applied the method described in Section V to reconstruct a Gaussian scalar field using 100 nodes, whose communication network either has a chain topology or a grid topology. The simulations were performed on a normalized domain of size 1 m $\times$ 1 m. The field was reconstructed using data collected over a time period of 50 sec from a set of 30 accessible nodes. Figure 2 and Figure 3 illustrate the results from using the chain and grid topologies, respectively. Each figure shows the contour plots of the actual field, the estimated field, and absolute value of the error between these plots. From these plots, it is evident that the grid topology yields a much more accurate reconstruction of the field than the chain topology, even though both networks can be characterized as observable.

In order to test the performance of our method in a practical scenario, we applied it in simulation to a set of real salinity data (psu), obtained from [29], over a section of the Atlantic Ocean at a depth of 25 m. The salinity field was reconstructed over a time period of 50 sec using 100 nodes with a grid communication topology and 30 accessible nodes whose temporal data were sampled at 10 Hz. During the simulation, each node measured the salinity at its position and transmitted this information to its neighboring nodes according to Equation (2). The temporal observations by the

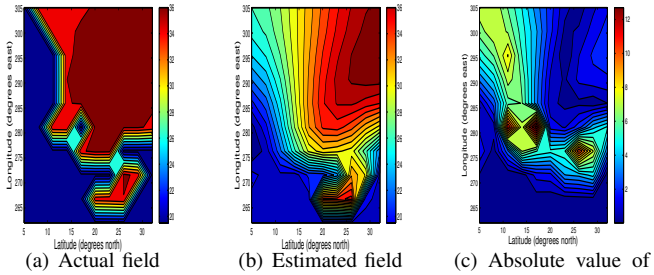

(a) Actual field (b) Estimated field (c) Absolute value of error

Fig. 4. Estimation of salinity (psu) over a section of the Atlantic Ocean at a depth of 25 m. The network consists of 100 nodes with a grid communication topology. Temporal data is acquired from 30 nodes over a time period of 50 sec.

accessible nodes, obtained over 50 sec according to Equation (3), were used to reconstruct the salinity measurements taken by all the nodes using the techniques described in Section V. The contour plots in Figure 4 show that the estimated salinity field reproduces the key features of the actual field with reasonable accuracy.

VII. EFFECT OF NETWORK TOPOLOGY ON ESTIMATION PERFORMANCE

In this section, we analyze the effect of network topology on the accuracy of the field estimation as the number of nodes in the network increases. Comparing the results in Figure 2 and Figure 3, it is evident that there is some fundamental limitation arising from the network structure which makes the system with the chain topology practically unobservable. In the control theory literature, the *degree of observability* is used as a metric of a system's observability [15]. The *observability Gramian* $W_O(0,T)$ can be used to compute the initial state of an observable linear system from output data over time $t \in [0\ T]$ [7]. This makes it a good candidate for use in quantifying the relative observability among different systems. Due to the duality of controllability and observability, the results associated with one of these properties can be used for the other if interpreted properly. Commonly used measures of the degree of observability (controllability) are the smallest eigenvalue, the trace, the determinant, and the condition number of the observability (controllability) Gramian [12], [13], [14]. For large, sparse networked systems, the Gramian can be highly ill-conditioned, which makes numerical computation of its minimum eigenvalue unstable. Although researchers have computed bounds on the minimum eigenvalues of the Gramian [11], these bounds did not help to us arrive at a conclusion since they were too close together.

These factors prompted us to use the trace of the observability Gramian as our metric for the degree of observability. Analogous to the interpretation of the controllability Gramian in [11], the trace of the observability Gramian can be interpreted as the average sensing effort applied by a system to estimate its initial state. For a communication network represented by $\mathscr{G}$ with information flow dynamics given by

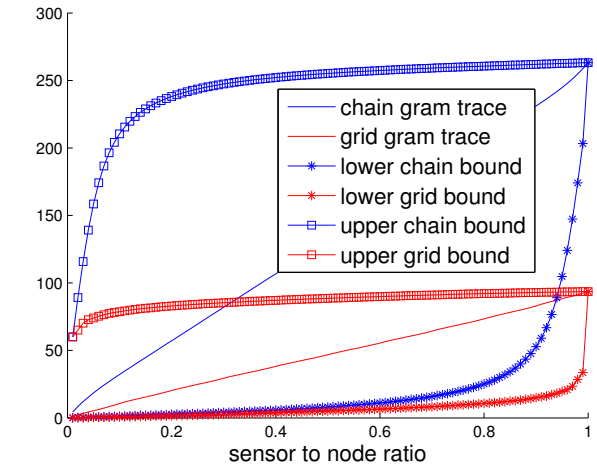

(a) Networks with 100 nodes

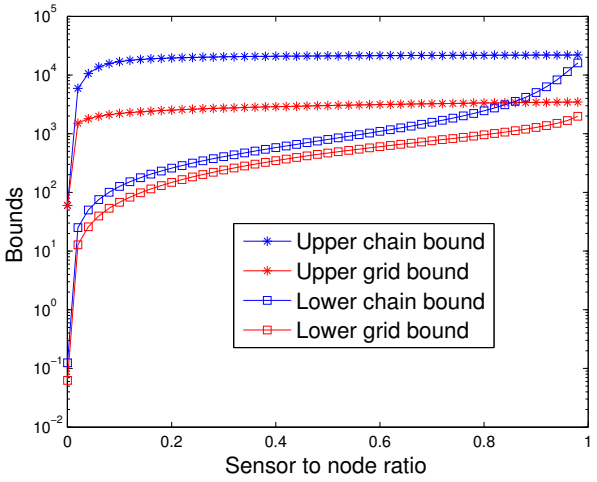

(b) Networks with 10000 nodes

Fig. 5. Comparison of the degree of observability based on the trace of the observability Gramian and its bounds. The trace shown in Figure 5(a) is computed numerically using the eigenvectors of $\mathbf{L}(\mathscr{G})$.

Equation (2), the trace of the observability Gramian $W_O(0,T)$ is defined as

$$Trace(W_O(0,T)) = Trace\left(\int_0^T \mathbf{e}^{-\mathbf{L}(\mathscr{G})^* t}\mathbf{C}^*\mathbf{C}\mathbf{e}^{-\mathbf{L}(\mathscr{G})t}dt\right). \tag{12}$$

Following steps similar to those in [11], we use Theorem 1 below to derive upper and lower bounds on the trace of the observability Gramian for networks with chain and grid topologies. Figure 5 compares these lower and upper bounds for two network sizes as a function of the sensor-to-total-node ratio, where the *sensors* are defined as the accessible nodes. It is clear from the plots that the average sensing effort required by the chain network is greater than that of the grid network for a given measurement energy, which is defined as $\|\mathbf{Y}(t)\|^2_{L^2([0\ T],\mathbb{R}^k)}$ [11], where $\mathbf{Y}(t)$ is obtained from Equation (3).

Theorem 1: Let $\mathscr{G}$ be an unweighted, undirected graph that represents the communication network of a set of N nodes with information dynamics and output map given by Equation (2) and Equation (3), respectively. If we label $V(\mathscr{G})$ such that $k \leq N$ sensor nodes in $V(\mathscr{G})$ are labeled as $1,2,...,k$, then $\mathbf{C} = \left[\mathbf{I}_{k\times k}\ \mathbf{0}_{k\times(N-k)}\right]$. Assuming that $\mathbf{L}(\mathscr{G})$ is diagonalizable and that $\lambda_1 \geq \lambda_2 \geq ... \geq \lambda_N$ are its eigenvalues, there exist real constants $c_1 \leq c_2 \leq ... \leq c_N$ such that

$$\sum_{i=1}^{k} c_i \ \leq \ Trace\left(W_O(0,T)\right) \ \leq \ \sum_{i=0}^{k-1} c_{N-i}, \tag{13}$$

where $c_i = \int_0^T e^{-2\lambda_i t} dt$.

Proof: From the definition of the trace operator, it can be shown that the trace and integral operators are commutative. Using this property and the property that the trace operator is invariant under cyclic permutation [30], Equation (12) can be written as

$$\begin{aligned} &Trace(W_O(0,T)) \\ &\quad = \int_0^T Trace\left(\mathbf{e}^{-\mathbf{L}(\mathscr{G})^* t}\mathbf{C}^*\mathbf{C}\mathbf{e}^{-\mathbf{L}(\mathscr{G})t}\right) dt \\ &\quad = \int_0^T Trace\left(\mathbf{C}^*\mathbf{C}\mathbf{e}^{\left(-\mathbf{L}(\mathscr{G})t - \mathbf{L}(\mathscr{G})^* t\right)}\right) dt. \end{aligned}$$

Since the Laplacian of an unweighted, undirected graph is a Hermitian matrix, this equation becomes

$$Trace(W_O(0,T)) = \int_0^T Trace\left(\mathbf{C}^*\mathbf{C}\mathbf{e}^{-2\mathbf{L}(\mathscr{G})t}\right) dt.$$

Let $\mathbf{L}(\mathscr{G}) = \mathbf{V}\Lambda\mathbf{V}^*$ such that $\Lambda = Diag(\lambda_1, \lambda_2, ..., \lambda_N)$ and the columns of $\mathbf{V} \in \mathbb{R}^{N\times N}$ are given by the corresponding eigenvectors of $\mathbf{L}(\mathscr{G})$. Then using the decomposition of the matrix exponential [27], the equation becomes

$$\begin{aligned} Trace(W_O(0,T)) &= \int_0^T Trace\left(\mathbf{C}^*\mathbf{C}\mathbf{V}\mathbf{e}^{-2\Lambda t}\mathbf{V}^*\right) dt \\ &= Trace\left(\mathbf{C}^*\mathbf{C}\mathbf{V}\left(\int_0^T \mathbf{e}^{-2\Lambda t} dt\right)\mathbf{V}^*\right). \end{aligned}$$

The matrix exponential $\int_0^T \mathbf{e}^{-2\Lambda t} dt$ is a diagonal matrix given by $Diag\left(\int_0^T \mathbf{e}^{-2\lambda_1 t} dt, \int_0^T \mathbf{e}^{-2\lambda_2 t} dt, ..., \int_0^T \mathbf{e}^{-2\lambda_N t} dt\right)$. We define $c_i = \int_0^T \mathbf{e}^{-2\lambda_i t} dt$. Then, since $\lambda_1 \geq \lambda_2 \geq ... \geq \lambda_N$, by definition we have that $c_1 \leq c_2 \leq ... \leq c_N$.

Let $\mathbf{M} = \mathbf{V}\left(\int_0^T \mathbf{e}^{-2\Lambda t} dt\right)\mathbf{V}^*$. Then we see that $\mathbf{M}$ is a Hermitian matrix with eigenvalues $c_1, c_2, ..., c_N$ and the same eigenvectors as $\mathbf{L}(\mathscr{G})$. Also, we find that $\mathbf{C}^*\mathbf{C}$ is a diagonal matrix with the first k diagonal elements equal to 1 and the rest equal to 0. Defining $\mathbf{P} = \mathbf{C}^*\mathbf{C}$, we obtain a compact form for the trace of the observability Gramian,

$$Trace\left(W_O(0,T)\right) = Trace\left(\mathbf{PM}\right). \tag{14}$$

Equation (14) can be reduced to:

$$Trace\left(W_O(0,T)\right) = Trace\left(\mathbf{PM}\right) = \sum_{i=1}^{k} M_{ii},$$

where M_{ii} denotes the i^{th} diagonal entry of $\mathbf{M}$.

From Theorem 1 of [31], we obtain the following lower bound:

$$Trace\left(W_O(0,T)\right) = \sum_{i=1}^{k} M_{ii} \ \geq \ \sum_{i=1}^{k} c_i. \tag{15}$$

Now by applying *Von Neumann's trace inequality* [30] to Equation (14) and the fact that $W_O(0,T)$ is at least positive semidefinite, we find that

$$Trace\left(\mathbf{PM}\right) \ \leq \ \sum_{i=0}^{n-1} \sigma\left(\mathbf{P}\right)_{n-i} \sigma\left(\mathbf{M}\right)_{n-i}$$

where $\sigma(\cdot)_i$ is the i^{th} singular value of a matrix. The singular values are arranged in increasing order, $\sigma(\cdot)_1 \leq \sigma(\cdot)_2 \leq ... \leq \sigma(\cdot)_N$, and here they coincide with the eigenvalues of the matrices. Note that only the last k eigenvalues of $\mathbf{P}$ are nonzero and are equal to 1. Thus, we obtain the upper bound:

$$Trace\left(W_O(0,T)\right) \ \leq \ \sum_{i=0}^{k-1} c_{N-i}. \tag{16}$$

■

Since we can obtain the eigenvalues of $\mathbf{L}(\mathscr{G}_c)$ and $\mathbf{L}(\mathscr{G}_g)$ analytically [18], we can use Theorem 1 to analyze and compare the scaling properties of the chain and grid network topologies in a more precise fashion. For each type of network, we specify that k of the N total nodes in the network are sensors (accessible nodes), where $k < \sqrt{N}$. Without loss of generality, we assume that the grid is square to simplify the analysis. By Theorem 1, the upper bound on $Trace\left(W_O(0,T)\right)$ is given by $\sum_{i=0}^{k-1} c_{N-i}$, where $c_{N-i} = \int_0^T e^{-2\lambda_{N-i} t} dt$. Let λ_{N-i}^c and λ_{N-i}^g denote the $(N-i)^{th}$ eigenvalue of $\mathbf{L}(\mathscr{G}_c)$ and $\mathbf{L}(\mathscr{G}_g)$, respectively. Then from [18], $\lambda_{N-i}^c = 4\sin^2\left(\frac{\pi i}{2N}\right)$ and $\lambda_{N-i}^g = 4\sin^2\left(\frac{\pi i}{2\sqrt{N}}\right)$ for $i \in \{0,1,...,k-1\}$. Since $k < \sqrt{N}$ implies that $\frac{k}{N} < \frac{1}{\sqrt{N}}$, for networks with large N we have that $\lambda_{N-i}^c \approx (\frac{\pi i}{N})^2$ and $\lambda_{N-i}^g \approx (\frac{\pi i}{\sqrt{N}})^2$. Therefore, the upper bound on $Trace\left(W_O(0,T)\right)$ for the chain network is given by:

$$\sum_{i=0}^{k-1} c_{N-i}^c \ = \ \sum_{i=0}^{k-1} \int_0^T e^{-2\frac{\pi^2 i^2}{N^2} t} dt, \tag{17}$$

which can be simplified to

$$\sum_{i=0}^{k-1} c_{N-i}^c \ = \ T + \frac{N^2}{2\pi^2}\left(\sum_{i=1}^{k-1} \frac{1 - e^{-2\frac{\pi^2 i^2}{N^2} T}}{i^2}\right). \tag{18}$$

Similarly, the upper bound on $Trace\left(W_O(0,T)\right)$ for the grid network can be reduced to:

$$\sum_{i=0}^{k-1} c_{N-i}^g \ = \ T + \frac{N}{2\pi^2}\left(\sum_{i=1}^{k-1} \frac{1 - e^{-2\frac{\pi^2 i^2}{N} T}}{i^2}\right). \tag{19}$$

From Equation (18) and Equation (19), we observe that the upper bound on the average sensing effort required by the chain network scales quadratically with the total number of nodes N, whereas this upper bound for the grid network scales linearly with N.

VIII. EFFECT OF NETWORK TOPOLOGY ON ROBUSTNESS TO NOISE

In this section, we analyze the effect of noise on the output of first-order linear dynamics that evolve on chain and grid network topologies. We assume that the data at each node in the network is affected by white noise with zero mean and unit covariance. Therefore, the augmented system dynamics described by Equation (2) can be written as

$$\dot{\mathbf{X}}(t) = -\mathbf{L}(\mathscr{G})\mathbf{X}(t) + W, \tag{20}$$

where $W \in \mathbf{R}^N$ denotes a zero mean, unit covariance white noise process. The output equation is the same as Equation (3).

As defined in the robust control literature, the $\mathscr{H}_2$ norm of a system gives the steady-state variance of the output when the input to the system is white noise and when $-\mathbf{L}(\mathscr{G})$ is Hurwitz [32]. However, for unstable systems, the finite steady-state variance can be computed only when the unstable modes are unobservable from the outputs [33]. For $\mathbf{L}(\mathscr{G})$, zero is the only unstable mode with corresponding eigenvector $\mathbf{1}_N$, which does not affect the steady-state variance of the output. If we can make the zero mode unobservable, then it is still possible to use the $\mathscr{H}_2$ norm as a measure to quantify the effect of noise on the system output.

In order to do so, we follow the approach in [34], which uses the *first-order Laplacian energy*. This quantity is essentially the $\mathscr{H}_2$ norm of a system if the matrix $\mathbf{C}$ in Equation (3) is chosen in such a way that it annihilates the vector $\mathbf{1}_N$. This can be done by defining $\mathbf{C}$ to be an incidence matrix of a graph $\mathscr{G}_k$. Denoting this new $\mathbf{C}$ by $\hat{\mathbf{C}}$, we have that $\mathbf{L}(\mathscr{G}_k) = \hat{\mathbf{C}}^T\hat{\mathbf{C}}$. Then $\mathbf{L}(\mathscr{G}_k)\mathbf{1}_N = 0$, which implies that $\hat{\mathbf{C}}\mathbf{1}_N = 0$ since $ker(\hat{\mathbf{C}}) = ker(\hat{\mathbf{C}}^T\hat{\mathbf{C}})$. Note that $\hat{\mathbf{C}}$ need not necessarily be the incidence matrix of a graph $\mathscr{G}_k$; the only condition required is that $\hat{\mathbf{C}}^T\hat{\mathbf{C}} = \mathbf{L}(\mathscr{G}_k)$.

Now, if $\mathscr{G}_k$ is chosen to be a weighted complete graph $\mathscr{K}_N$ whose edges all have weight $\frac{1}{N}$, then $\mathbf{L}(\mathscr{G}_k) = \mathbf{I}_{N\times N} - \frac{1}{N}\mathbf{J}_N$. The first-order Laplacian energy, $\mathscr{H}^{(1)}_{\mathscr{K}_N}(\mathbf{L}(\mathscr{G}))$, for the corresponding $\mathbf{C}$ can be defined from [34] as

$$\mathscr{H}^{(1)}_{\mathscr{K}_N}(\mathbf{L}(\mathscr{G})) = \sum_{i=1}^{N-1} \frac{1}{2\lambda_i}, \tag{21}$$

where $\lambda_1 \geq \lambda_2 \geq \ldots \geq \lambda_N = 0$ are the eigenvalues of $\mathbf{L}(\mathscr{G})$.

In Figure 6, we compare $\mathscr{H}^{(1)}_{\mathscr{K}_N}(\mathbf{L}(\mathscr{G}))$ for graphs with grid and chain network topologies as a function of the total number of nodes in the network. The plot shows that the grid network is more effective than the chain network at mitigating the effect of noise on the system output for a given number of nodes.

IX. CONCLUSION

In this work, we have presented a methodology to estimate the initial state of a large networked system of nodes with first-order linear information dynamics using output measurements from a subset of the nodes. We have quantified the advantages of a grid network over a chain network in the estimation of a two-dimensional scalar field, even though both networks can be made observable by construction. We have also used a performance measure based on the $\mathscr{H}_2$ norm of the network to characterize the robustness of the network dynamics based on its structure. A straightforward extension of this work is to compare the chain and grid topologies with similar degree distributions using the same methodology. Another interesting aspect to investigate is the effect of structural uncertainty in the networks, which could be done by quantifying the observability radius of the networks, as defined in [35]. In addition, we would like to compare network topologies in an alternative way by viewing $\mathbf{L}(\mathscr{G}_c)$ and $\mathbf{L}(\mathscr{G}_g)$ as approximations to the Laplace operator for 1D and 2D heat equations and analyzing the Gramians of these partial differential equations [36].

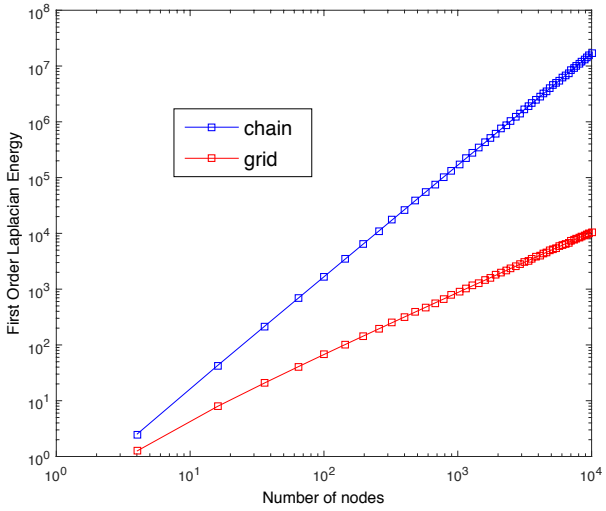

Fig. 6. Performance measure based on the first-order Laplacian energy.

ACKNOWLEDGMENT

R.K.R. thanks Karthik Elamvazhuthi for his valuable input on this work, especially regarding the change of variables in the derivation of the gradient.

REFERENCES

[1] S. S. Iyengar and R. R. Brooks, *Distributed Sensor Networks: Sensor Networking and Applications*. CRC press, 2012.

[2] A. Ahmad, G. D. Tipaldi, P. Lima, and W. Burgard, "Cooperative robot localization and target tracking based on least squares minimization," in *IEEE Int'l. Conference on Robotics and Automation (ICRA)*, 2013, pp. 5696–5701.

[3] S. Pequito, S. Kruzick, S. Kar, J. M. Moura, and A. Pedro Aguiar, "Optimal design of distributed sensor networks for field reconstruction," in *Proc. of the European Signal Processing Conference (EUSIPCO)*. IEEE, 2013, pp. 1–5.

[4] J. P. Desai, J. P. Ostrowski, and V. Kumar, "Modeling and control of formations of nonholonomic mobile robots," *IEEE Trans. on Robotics and Automation*, vol. 17, no. 6, pp. 905–908, 2001.

[5] G. Antonelli and S. Chiaverini, "Kinematic control of platoons of autonomous vehicles," *IEEE Trans. on Robotics*, vol. 22, no. 6, pp. 1285–1292, 2006.

[6] J. Kasac, V. Milic, B. Novakovic, D. Majetic, and D. Brezak, "Initial conditions optimization of nonlinear dynamic systems with applications to output identification and control," in *Mediterranean Conf. on Control & Automation (MED)*. IEEE, 2012, pp. 1247–1252.

[7] J. P. Hespanha, *Linear System Theory*, 1st ed. Princeton, NJ, USA: Princeton University Press, 2009.

[8] Y.-Y. Liu, J.-J. Slotine, and A.-L. Barabási, "Observability of complex systems," *Proc. of the National Academy of Sciences*, vol. 110, no. 7, pp. 2460–2465, 2013. [Online]. Available: http://www.pnas.org/content/110/7/2460.abstract

[9] M. Ji and M. Egerstedt, "Observability and estimation in distributed sensor networks," in *IEEE Conf. on Decision and Control (CDC)*, Dec. 2007, pp. 4221–4226.

[10] Z. Yuan, C. Zhao, Z. Di, W.-X. Wang, and Y.-C. Lai, "Exact controllability of complex networks," *Nat. Commun.*, vol. 4, Sept 2013. [Online]. Available: http://dx.doi.org/10.1038/ncomms3447

[11] F. Pasqualetti, S. Zampieri, and F. Bullo, "Controllability metrics and algorithms for complex networks," *CoRR*, vol. abs/1308.1201, 2013. [Online]. Available: http://arxiv.org/abs/1308.1201

[12] F. Pasqualetti and S. Zampieri, "On the controllability of isotropic and anisotropic networks," in *IEEE Conf. on Decision and Control (CDC)*, Dec 2014, pp. 607–612.

[13] G. Yan, G. Tsekenis, B. Barzel, J.-J. Slotine, Y.-Y. Liu, and A.-L. Barabási, "Spectrum of controlling and observing complex networks," *Nat. Phys.*, vol. 11, no. 9, pp. 779–786, Sep 2015, article. [Online]. Available: http://dx.doi.org/10.1038/nphys3422

[14] C. Enyioha, M. A. Rahimian, G. J. Pappas, and A. Jadbabaie, "Controllability and fraction of leaders in infinite network," *CoRR*, vol. abs/1410.1830, 2014. [Online]. Available: http://arxiv.org/abs/1410.1830

[15] P. C. Müller and H. I. Weber, "Analysis and optimization of certain qualities of controllability and observability for linear dynamical systems," *Automatica*, vol. 8, no. 3, pp. 237–246, May 1972. [Online]. Available: http://dx.doi.org/10.1016/0005-1098(72)90044-1

[16] G. Notarstefano and G. Parlangeli, "Controllability and observability of grid graphs via reduction and symmetries," *IEEE Trans. on Automatic Control*, vol. 58, no. 7, pp. 1719–1731, July 2013.

[17] G. Parlangeli and G. Notarstefano, "On the reachability and observability of path and cycle graphs," *IEEE Trans. on Automatic Control*, vol. 57, no. 3, pp. 743–748, March 2012.

[18] T. Edwards, "The discrete Laplacian of a rectangular grid," https://www.math.washington.edu/~reu/papers/2013/tom/Discrete%20Laplacian%20of%20a%20Rectangular%20Grid.pdf, August 2013.

[19] C. Godsil and G. Royle, *Algebraic Graph Theory*, ser. Graduate Texts in Mathematics. New York: Springer-Verlag, 2001, vol. 207. [Online]. Available: http://dx.doi.org/10.1007/978-1-4613-0163-9

[20] M. Mesbahi and M. Egerstedt, *Graph Theoretic Methods for Multiagent Networks*, 1st ed. Princeton, NJ, USA: Princeton University Press, Sept. 2010.

[21] T. Banham, "The discrete Laplacian and the hotspot conjecture," https://www.math.washington.edu/~reu/papers/2006/tim/laplace.pdf, August 2006.

[22] R. C. Wilson and P. Zhu, "A study of graph spectra for comparing graphs and trees," *Pattern Recognition*, vol. 41, no. 9, pp. 2833 – 2841, 2008. [Online]. Available: http://www.sciencedirect.com/science/article/pii/S0031320308000927

[23] S. Boyd and L. Vandenberghe, *Convex Optimization*. New York, NY, USA: Cambridge University Press, 2004.

[24] D. G. Luenberger, *Optimization by Vector Space Methods*, 1st ed. New York, NY, USA: John Wiley & Sons, Inc., 1997.

[25] M. Hochbruck and C. Lubich, "On Krylov subspace approximations to the matrix exponential operator," *SIAM Journal on Numerical Analysis*, vol. 34, no. 5, pp. 1911–1925, 1997. [Online]. Available: http://dx.doi.org/10.1137/S0036142995280572

[26] L. Orecchia, S. Sachdeva, and N. K. Vishnoi, "Approximating the exponential, the Lanczos method and an $\tilde{O}(m)$-time spectral algorithm for balanced separator," in *Proc. of the ACM Symposium on Theory of Computing*, ser. STOC '12. New York, NY, USA: ACM, 2012, pp. 1141–1160. [Online]. Available: http://doi.acm.org/10.1145/2213977.2214080

[27] G. Strang, *Linear Algebra and Its Applications*, 3rd ed. NY, USA: Brooks/Cole, 1988.

[28] C. Moler and C. V. Loan, "Nineteen dubious ways to compute the exponential of a matrix, twenty-five years later," *SIAM Review*, vol. 45, no. 1, pp. 3–49, 2003. [Online]. Available: http://dx.doi.org/10.1137/S00361445024180

[29] National Centers for Environment Information, "Salinity of Atlantic ocean," http://ecowatch.ncddc.noaa.gov/thredds/catalog/amseas/catalog.html, Sept. 2015.

[30] R. A. Horn and C. R. Johnson, Eds., *Matrix Analysis*. New York, NY, USA: Cambridge University Press, 1986.

[31] J. Daboul, "Inequalities among partial traces of Hermitian operators and partial sums of their eigenvalues," Ph.D. dissertation, Ben Gurion University of the Negev, 1990.

[32] G. E. Dullerud and F. G. Paganini, *A course in robust control theory: A convex approach*, ser. Texts in Applied Mathematics. New York, NY, USA: Springer, 2000. [Online]. Available: http://opac.inria.fr/record=b1098305

[33] B. Bamieh, M. R. Jovanović, P. Mitra, and S. Patterson, "Coherence in large-scale networks: dimension dependent limitations of local feedback," *IEEE Trans. on Automatic Control*, vol. 57, no. 9, pp. 2235–2249, Sept. 2012.

[34] M. Siami and N. Motee, "Graph-theoretic bounds on disturbance propagation in interconnected linear dynamical networks," *arXiv preprint arXiv:1403.1494*, 2014.

[35] G. Bianchin, P. Frasca, A. Gasparri, and F. Pasqualetti, "The observability radius of network systems," in *American Control Conference (ACC)*, Boston, MA, USA, 2016, pp. 185–190.

[36] F. Van den Berg, H. Hoefsloot, H. Boelens, and A. Smilde, "Selection of optimal sensor position in a tubular reactor using robust degree of observability criteria," *Chemical Engineering Science*, vol. 55, no. 4, pp. 827–837, 2000.